Supplemental information for:

Sequential activation of human signal recognition particle by the ribosome and signal sequence drives efficient protein targeting

Jae Ho Lee[1], Sowmya Chandrasekar[1], SangYoon Chung[2], Yu-Hsien Hwang Fu[1], Demi Liu[1,3], Shimon Weiss[2,4], Shu-ou Shan[1]*

[1]Division of Chemistry and Chemical Engineering, California Institute of Technology, Pasadena, CA 91125

[2]Department of Chemistry and Biochemistry, University of California Los Angeles, Los Angeles, CA 90095

[3]Current address: Department of Chemistry, University of Washington – Seattle, Seattle, WA 98195

[4]Department of Physics, Institute of Nanotechnology and Advanced Materials, Bar-Ilan University, Ramat-Gan, 52900, Israel

* corresponding author. Email: sshan@caltech.edu

Supplemental Information includes Supplemental Methods, Supplemental Figures 1-7, and Supplemental Tables 1-2.

www.pnas.org/cgi/doi/10.1073/pnas.1802252115

Supplemental Methods

Vectors. pET15b-h19 and pET23d-h54 for expression of hSRP19 and hSRP54, respectively, were gifts from C. Zwieb (1, 2). pET3b-h9 and pET9a-h14 for expression of hSRP9 and hSRP14, respectively, and pS7CA for *in vitro* transcription of the 7SL SRP RNA were gifts from K. Strub (3, 4). pRS426-h68/72 vector and BCY123 yeast strain for expression of hSRP68/72 were gifts from K. Nagai (5). Commercially available cDNA clones for human SRα (Origene) and mouse SRβ (SINO Biological) were subcloned to construct pET28a-hSRα, pET15b-SRβΔTM, and bicistronic pET28a-hSRα-SRβΔTM using Gibson cloning for co-expression of hSRαβΔTM. The X-domain of SRα was removed from pET28a-hSRα using fastcloning to construct pET28a-hSRαΔX. Cyslite hSRP54, cysless hSRP19, and single cysteine mutants of hSRP54 and hSRP19 for fluorescence labeling were generated by QuikChange mutagenesis (Strategene). pET23d-h54-4A10L for expression of signal sequence fused hSRP54 was constructed using fastcloning. Sortase-tagged hSRαΔX was constructed by adding the sortase tag and $(GS)_6$ linker at the C-terminus using fastcloning.

Biochemical Preparations.

hSRP19. Rosetta pLysS cells harboring pET-h19 were grown to OD_{600} = 0.6 at 25 °C. Expression was induced with 1 mM IPTG for 16 hrs at 25 °C. Cells were resuspended in Lysis Buffer (50 mM KHEPES (pH 7.5), 300 mM NaCl, 10% glycerol, 4 mM βME, and protease inhibitor cocktail (ProBlock Gold (Gold Bio), 1X)) and lysed by two passes through French press at 18,000 psi. Clarified lysate was incubated for 1 hr with Ni-NTA resin (2ml/L of cells) equilibrated with Lysis Buffer. The resin was washed with 20 CV of Wash buffer (50 mM KHEPES (pH 7.5), 1 M NaCl, 5% glycerol, and 4 mM βME) containing 10 mM Imidazole, and protein was eluted with Lysis buffer supplemented with 250 mM Imidazole. Eluted protein was dialyzed in SP Buffer (50 mM Tris-HCl (pH 7.5), 150 mM NaCl, 2 mM EDTA, 5% glycerol, and 2mM DTT), and further purified over SP-sepharose ion-exchange column using a gradient of 150–500mM NaCl over 20CV. Purified hSRP19 was stored in 20% glycerol at –80°C.

hSRP9/14. hSRP9 and hSRP14 were expressed separately in BL21(DE3) pLysS cells grown in LB media with 0.4% glucose at 37 °C. Expression was induced at OD_{600} = 0.6 using 0.4 mM IPTG for 3 hours. Cells were resuspended in Lysis buffer (50 mM Tris-HCl (pH 7.5), 50 mM NaCl, 0.25 M NH_4Cl, 10 mM $MgCl_2$, 20 mM EDTA, 10% glycerol, 10 mM DTT, and 2 mM AEBSF) and lysed by sonication. Clarified lysate containing SRP9 and SRP14 were mixed at 1:1 ratio and stirred gently for 30 minutes. The mixture was loaded onto Heparin-sepharose resin (10 ml/L of cells) equilibrated with Heparin Buffer (50 mM KHEPES (pH 7.5), 50 mM NaCl, 0.25 M NH_4Cl, 1 mM EDTA, 10% glycerol, 10 mM DTT, and 2 mM AEBSF). The resin was washed with 10 CV of Heparin Buffer with 250 mM KOAc. Proteins were eluted using a gradient of 250 mM – 1.5 M KOAc. Peak fractions were dialyzed in Buffer A (50 mM KHEPES (pH 7.5), 300 mM KOAc, 1 mM EDTA, 0.01% Nikkol, 10% glycerol, 10 mM DTT, and 1 mM AEBSF) and further purified over a MonoS cation-exchange column using a gradient of 300 mM – 650 mM KOAc over 20CV. Purified hSRP9/14 was stored in 20% glycerol at –80°C.

hSRP54. *h*SRP54 or hSRP54-4A10L were expressed in Rosetta pLysS cells grown at 37 °C to OD_{600} = 0.6. Cells were chilled to 25 °C in a water bath for 15 minutes, and expression was induced using 1 mM IPTG for 2 hours at 25 °C. Cells were resuspended in Lysis Buffer (50 mM KHEPES (pH 7.5), 100 mM NaCl, 4 mM βME, 1 mM AEBSF, and Protease Inhibitor cocktail) and lysed by sonication. Clarified lysate was incubated with Ni-Sepharose resin (1.5 ml/L of cells) equilibrated in Lysis Buffer for 1 hr. The resin was washed with 20CV of Ni-buffer (50 mM KHEPES (pH 7.5), 500 mM NaCl, 40 mM Imidazole, 10% glycerol, 4 mM βME, and 1 mM AEBSF). Protein was eluted with Lysis buffer containing 300 mM NaCl and 300 mM Imidazole. Eluted protein was dialyzed to MonoS buffer (50 mM Tris-HCl (pH 7.5), 2 mM EDTA, 10% glycerol, and 2 mM DTT) with 150 mM NaCl, and purified over a MonoS column using a gradient of 150–600 mM NaCl over 20CV. Purified hSRP54 or hSRP54-4A10Lwas stored in 20% glycerol at –80°C.

hSRP68/72. hSRP68 and C-terminally His_6-tagged hSRP72 were co-expressed in BCY123 yeast cells grown in SD-Ura + 2% glucose media at 30 °C. 25 mL of this culture was inoculated into 1L of SD-

Ura + 2% raffinose media and cells were grown to OD_{600} = 0.9. Expression was induced by adding 2% galactose for 16 hours. Cells were washed twice with ice-cold water and flash frozen in droplets. Frozen cells were ground to powder in liquid nitrogen using Cryomill (Retsch), and mixed with Lysis buffer (50 mM K-Phosphate (pH 7.4), 1 M NaCl, 0.5 M Urea, 4 mM βME, 10% glycerol, and Protease inhibitor cocktail), and centrifuged at 42,000rpm in Ti45 rotor for 40 minutes. Clarified lysate was incubated with Ni-Sepharose resin (1.5ml/L of cells) equilibrated in Equilibration buffer (50 mM K-Phosphate (pH 7.4), 500 mM NaCl, 0.5 M Urea, 4 mM βME, and 10% glycerol) for 1 hour. The resin was washed with 20CV of Equilibration buffer containing 35 mM imidazole. Protein was eluted using Equilibration buffer containing 500 mM Imidazole, and eluted hSRP68/72 was further purified over a MonoS column using a gradient of 0.5 – 1 M NaCl over 20CV. Purified hSRP68/72 was stored in 50% glycerol at –30°C.

hSRαβΔTM and hSRαΔX. To express hSRαβΔTM, pET28 vector encoding N-terminally His_6-tagged hSRα and hSRβΔTM [hSRβ(57-269)], and pET15 vector encoding hSRβΔTM were co-transformed into BL21(DE3*). For hSRαΔX, pET28 vector encoding N-terminally His_6-tagged hSRαΔX [hSRα(131-638)] was transformed into BL21(DE3*). Cells were grown at 30 °C to OD_{600} = 0.6, and expression was induced with 0.5 mM IPTG for 4 hours. Cells were resuspended in Lysis Buffer (50 mM KHEPES (pH 8.0), 500 mM NaCl, 10% glycerol, 4 mM βME, and protease inhibitor cocktail) and lysed by two passages through French press at 18,000 psi. Clarified lysate was incubated with Ni-Sepharose resin (3 ml/L of cells) equilibrated in Lysis Buffer for 1 hr. The resin was washed with 15CV of Wash Buffer (50 mM KHEPES (pH 7.5), 500 mM NaCl, 35 mM Imidazole, 10% glycerol, and 4 mM βME). Bound protein was eluted with Wash Buffer containing 500 mM imidazole. Fractions containing target protein were diluted to 60 mM NaCl with Dilution Buffer (50mM KHEPES (pH 8.0) and 20% glycerol) and incubated with CM-Sepharose resin (5ml/L of cells) equilibrated in CM Buffer (50 mM KHEPES (pH 8.0), 10% glycerol, and 2 mM DTT) containing 100 mM KOAc for 1hr. The resin was washed with 10CV of CM-Buffer containing 100 mM KOAc, and protein was eluted with CM Buffer containing 350 mM KOAc. Peak fractions were pooled, concentrated, and further purified on a Superdex200 size-

exclusion column in S200 Buffer (50 mM KHEPES (pH 7.5), 300 mM KOAc, 5 mM $Mg(OAc)_2$, 10% glycerol, 0.02% Nikkol, and 2 mM DTT). Purified hSR was stored in 20% glycerol at –80 °C.

SRP RNA. S7CA, a circularly permutated version of human 7SL SRP RNA for improved SRP assembly, was *in vitro* transcribed using T7 RNA polymerase as described (4). Transcribed RNA was acid phenol extracted and purified over a denaturing polyacrylamide gel (100 mM Tris, 89 mM Boric Acid, 1.3 mM EDTA, 7 M Urea, and 10% acrylamide(29:1)) (6). RNA extracted from the gel was dialyzed in 20 mM Tris-HCl (pH 7.5), flash frozen in liquid nitrogen, and stored at –80 °C.

80S purification. Rabbit Reticulocyte Lysate (RRL) was treated with micrococcal nuclease (Nuclease S7; Roche) as described before (7). 20 mL nuclease treated RRL was ultracentrifuged at 42,000 rpm on TI70 rotor for 3.5 hours. The ribosome pellet was carefully resuspended with 6 mL HS Buffer (50 mM KHEPES (pH 7.5), 500 mM KOAc, 10 mM $Mg(OAc)_2$, and 2 mM DTT) and layered on 1M sucrose cushion (1M Sucrose in HS Buffer) and centrifuged at 95,000 rpm in a TLA100.3 rotor for 90 minutes. The ribosome pellet was resuspended with 6ml of HS Buffer and 1ml sample was layered on a 40 ml 10–50% sucrose gradient in HS Buffer. The gradient was ultracentrifuged at 23,000 rpm in a SW32 rotor for 12 hours. The monosome peak was collected and centrifuged at 95,000 rpm in a TLA100.3 rotor for 90 minutes. The ribosome pellet was gently washed once with SRP Assay buffer, and resuspended in SRP Assay buffer without Nikkol to desired concentration. Aliquots were flash frozen in liquid nitrogen and stored at –80 °C.

RNC purification. mRNA encoding the nascent chains on RNC was translated in Rabbit Reticulocyte Lysate for 30 minutes at 32 °C (8). 1.8 mL of translation reactions was layered on a 1 mL 0.5M Sucrose cushion (50 mM KHEPES (pH 7.1), 100 mM KOAc, 15 mM $Mg(OAc)_2$, 0.5 M Sucrose, 0.1% Triton, and 20 μg/ml Cycloheximide) and centrifuged at 100,000 rpm for 1 hour at 4 °C in a TLA100.3 rotor. The pellet was resuspended with Resuspension Buffer (50 mM KHEPES (pH 7.1), 100 mM KOAc, 15 mM $Mg(OAc)_2$, and 20 μg/ml Cycloheximide) and incubated with anti-FLAG resin (anti-FLAG M2 Magnetic Beads (Sigma), 5 μL/mL translation) for 1-2 hours. The resin was washed with 20

CV of Wash 1 Buffer (50 mM KHEPES (pH 7.1), 100 mM KOAc, 15 mM $Mg(OAc)_2$, 0.1% Triton, and 20 μg/ml Cycloheximide) followed by 20 CV of Wash 2 Buffer (50 mM KHEPES (pH 7.1), 300 mM KOAc, 15 mM $Mg(OAc)_2$, and 20 μg/ml Cycloheximide). RNC was eluted three times with 2 CV of Elution Buffer (50 mM KHEPES (pH 7.1), 150 mM KOAc, 15 mM $Mg(OAc)_2$, 1 mg/ml 3xFLAG peptide, and 20 μg/ml Cycloheximide). Eluted RNCs were layered on a 4.8 mL 10–30 % sucrose gradient (in 50 mM KHEPES (pH 7.1), 500 mM KOAc, 10 mM $Mg(OAc)_2$, 2 mM DTT, 20 μg/ml Cycloheximide, and 0.3 mg/ml BSA) and ultracentrifuged at 50,000 rpm for 100 minutes at 4 °C in a SW55 rotor (9). 200 μL fractions were collected from the top of the gradient. The monosome peak fractions were combined and centrifuged at 95,000 rpm for 95 minutes at 4 °C in a TLA100.3 rotor. The RNC pellet was resuspended in SRP Assay Buffer, flash frozen in liquid nitrogen, and stored at –80°C.

Fluorescence labeling

hSRP54. There are five native cysteines in hSRP54. The three exposed cysteines in hSRP54 were mutated (C36T, C136S, and C229A) to generate 'cyslite' hSRP54, which did not show detectable labeling with maleimide dyes. An engineered cysteine (C47 or C12) was introduced into cyslite hSRP54 for site-specific labeling using maleimide chemistry (10). 50 μM hSRP54 or hSRP54-4A10L was treated with 2 mM TCEP for 4 hours at room temperature. A 15-fold excess of Cy3b (or ATTO 550 or ATTO 647N) maleimide was added and incubated at room temperature for 4 hours. Labeled protein was separated from free dye by size exclusion chromatography on a G-25 column (10). Labeled protein was concentrated and stored in 20% glycerol at –80°C. Labeling efficiency was 70–80%.

hSRP19. The native cysteines in hSRP19 were mutated (C3S, C17V, C53L, and C94S) to generate cysless hSRP19, into which a single cysteine (K64C) is introduced. 50 μM hSRP19 (K64C) was treated with 2 mM TCEP for 4 hours at room temperature. A 10-fold excess of ATTO 550 or ATTO 647N maleimide was added and incubated at room temperature for 2 hours. Labeled hSRP19 was

separated from free-dye by size exclusion on a G-25 column. Labeled protein was stored in 20% glycerol at –80°C. Labeling efficiency was ~80%.

hSR. A sortase-tag (LPETG) with $(GS)_6$ linker was added to the C-terminus of hSRαΔX (11). A sortase peptide (GGGC) was labeled with ATTO 647N via maleimide chemistry, and labeled peptide was purified by HPLC using a C18 column. To label SR, 1:4:8 molar ratio of sortase-tagged SRαΔX or SRαβΔTM, sortase, and labeled peptide was mixed in Sortase Buffer (50 mM Tris-HCl (pH 7.5), 150 mM NaCl, 10 mM $CaCl_2$, 10% glycerol, 1 mM DTT, and 0.02% Nikkol) and incubated for 3-4 hours at room temperature. The reaction mixture was purified on Ni-Sepharose resin to remove untagged-sortase and free peptides. Labeling efficiency was 60–70%. Labeled protein was concentrated and stored in 20% glycerol at –80°C.

Biochemical assays. All proteins except for SRP were centrifuged at 4 °C, 100,000 rpm in TLA100 rotor for 30 minutes to remove aggregates before the assay. GTPase reactions were performed in SRP Assay Buffer (50 mM KHEPES (pH 7.5), 150 mM KOAc, 5 mM $Mg(OAc)_2$, 10% glycerol, 2 mM DTT, and 0.04% Nikkol) at 25 °C. Reactions were followed and analyzed as described before (12) except that PEI cellulose thin layer chromatography were run in 1 M formic acid / 0.5 M LiCl. Observed rate constants were determined as described before (12).

Steady-state fluorescence measurements to analyze the SRP-SR interaction were carried out on a Fluorolog 3-22 spectrofluorometer (Jobin Yvon) and Kintek stopped-flow apparatus (Kintek Inc.) at 25 °C. The binding of SRP to RNC_{4A10L} or to 80S was measured using Microscale Thermophoresis (MST; Nanotemper) following manufacturer's instructions.

Co-translational targeting and translocation of ^{35}S-methionine labeled pPL into salt-washed, trypsinized rough ER microsome (TKRM) was measured in wheat germ extract as previously described (13, 14). The efficiency of translocation was quantified as:

$$\%\text{Translocation} = \frac{\left(\frac{8}{7}\right) prolactin}{\left(\frac{8}{7}\right) prolactin + preprolactin} \times 100$$

The (8/7) term here corrects for the different number of methionines in pPL versus signal sequence-cleaved prolactin.

Determination of individual rate and equilibrium constants. Basal GTPase reactions were measured under single-turnover conditions using varying concentrations of hSRP or hSR in excess of trace γ-^{32}P-GTP. The SRP or SR concentration dependence of the observed rate constant (k_{obsd}) were fit to Eq. 1,

$$k_{obsd} = k_{cat} \times \frac{[\text{SRP or SR}]}{K_m + [\text{SRP or SR}]} \qquad (1)$$

in which k_{cat} is basal GTPase rate constants and K_m is the GTP concentration required to reach half of the maximal observed GTPase rate constant.

The reciprocally stimulated GTPase reaction between SRP and SR were measured under multiple turnover conditions using 0.2 μM hSRP, varying concentrations of excess hSR, and 100 μM GTP doped with trace γ-^{32}P-GTP. The SR concentration dependences of observed rate constants were fit to Eq. 2.

$$k_{obsd} = k_{cat} \times \frac{[\text{SR}]}{K_m + [\text{SR}]} \qquad (2)$$

The binding affinity of GDP for hSRP and hSR were determined using GDP as a competitive inhibitor of the basal GTPase reaction. The GDP concentration dependence of observed rate constants were fit to Eq. 3,

$$k_{obsd} = k_0 \times \frac{K_i}{[\text{GDP}] + K_i} \qquad (3)$$

where k_0 is rate in the absence of GDP and K_i is inhibition constant.

Inhibition of GTPase activity by hSRαΔX(R458A) was measured in multi-turnover conditions using 0.2 μM of hSRP, 0.5 μM of hSRαΔX, and increasing concentrations of hSRαΔX(R458A). hSRαΔX(R458A) concentration dependence of observed rate constants were fit to Eq. 4,

$$k_{obsd} = k_0 \times \frac{[SR]}{[SR] + K_m \times (1 + \frac{[SR_{R458A}]}{K_i})} \qquad (4)$$

where k_0 is the observed reaction rate in the absence of hSRαΔX(R458A), [SR] = 0.5 μM, K_m is the Michaelis constant for the reaction of wildtype hSRP with SR, determined as 0.06 μM from the data in Figure 2, and K_i is the inhibition constant of hSRαΔX(R458A).

Association rate constants between hSRP and hSR were measured on a stopped-flow apparatus by rapid mixing of a fixed concentration of Cy3B-labeled hSRP or hSRP-4A10L with varying concentrations of excess ATTO-647N-labeled hSRαΔX. The time courses of fluorescence change were fit to exponential functions to extract the observed association rate constants (k_{obsd}). The SR concentration dependences of k_{obsd} values were fit to Eq. 5,

$$k_{obsd} = k_{on} \times [SR] + k_{off} \qquad (5)$$

in which k_{on} is the bi-molecular association rate constant between hSRP and hSR, and k_{off} is the dissociation rate constant of the hSRP•hSR complex. The ribosome or RNC was pre-incubated with hSRP where indicated.

The values of k_{off} were also directly determined using pulse chase experiments. Labeled hSRP and hSR were mixed and incubated until it reached equilibrium. Excess amount of unlabeled hSR was added to initiate chase, and the fluorescence signal change over time was measured. Resulting time-courses were fit to exponential functions to extract k_{off}.

Equilibrium titrations to measure the equilibrium dissociation constant (K_d) of the hSRP•hSR complex were carried out using 15 nM Cy3B labeled SRP, 2mM GTP, and addition of increasing

concentrations of ATTO-647N-labeled SR. Donor fluorescence was recorded when equilibrium is reached. 0.6 mg/ml BSA was supplemented in SRP Assay buffer to reduce non-specific adhesion of proteins to surfaces. A control titration with unlabeled hSR was carried out in parallel, and the fluorescence signal change from the control reaction was subtracted. The fluorescence signal was converted to FRET (E) using Eq. 6,

$$E = 1 - \frac{F_{DA}}{F_D} \qquad (6)$$

where F_{DA} and F_D are the fluorescence signals with and without the acceptor present. E was plotted against hSR concentration and fit to Eq. 7,

$$E = E_{max} \times \frac{[SR]}{K_d + [SR]} \qquad (7)$$

in which E_{max} is the value of E at saturating SR concentrations. Independently, the values of K_d were calculated from: $K_d = k_{off} / k_{on}$.

Equilibrium binding affinities between hSRP/hSRP-4A10L and 80S/RNCs were measured on Microscale Thermophoresis (MST) instrument (Nanotemper). 15 nM of Cy3B labeled hSRP/hSRP-4A10L was incubated with series of concentrations of either 80S or RNC_{4A10L}. Thermophoresis of each sample was measured and normalized fluorescence change was plotted against 80S/RNC4A10L concentration, and fit to Eq. 8,

$$\Delta F = \frac{[SRP] + [80S/RNC] + K_d - \sqrt{([SRP] + [80S/RNC] + K_d)^2 - 4[SRP] \times [80S/RNC]}}{2 \times [SRP]} \qquad (8)$$

where ΔF is normalized fluorescence, and K_d is equilibrium binding constant.

smFRET measurements.

All smFRET data analyses including burst search, burst selection were performed using FRETBursts, an open-source burst analysis toolkit for confocal smFRET (17). A dual-channel burst search (18) was performed to isolate the photon streams of particles containing FRET pairs from those containing only the donor or acceptor dye. Each burst (assumed to be the fluorescence signal from an individual SRP particle) was identified as a minimum of 10 consecutive detected photons with a photon count rate at least 10 times higher than the background photon count rate during both donor and acceptor excitation periods. Since the background rate can fluctuate within a measurement, the background rate was computed for every 50 second interval according to maximum likelihood fitting of the inter-photon delay distribution. The identified bursts were further selected according to the following criteria: (i) $n_{DD} + n_{DA} \geq 25$; and (ii) $n_{AA} \geq 25$, where n_{DD} and n_{DA} are the number of photons emitted from donor and acceptor during the donor excitation period, respectively, and n_{AA} is the number of photons emitted from acceptor during the acceptor excitation period.

The uncorrected FRET efficiency (E*) and the Stoichiometry (S) for each burst were calculated using the following equations:

$$E^* = \frac{n_{DA}}{n_{DD} + n_{DA}} \qquad (9)$$

$$S = \frac{n_{DD} + n_{DA}}{n_{DD} + n_{DA} + n_{AA}} \qquad (10)$$

In most cases, E* is different from the actual FRET efficiency due to simplifying assumptions (*i.e. lk=0*, *dir=0*, *γ=1)*. However, since the correction factors only depend on the photo-physical properties of fluorophores and the configuration of the optical setup, their contributions to the actual FRET efficiency are constant as long as the same optical set up, FRET pair and labeling position are used throughout all measurements. Importantly, we did not observe any significant changes in the photo-physical properties of both the donor and acceptor dyes by local environments (i.e. different conformations, substrates, ligands) (Fig. 6 and Fig. S7). Therefore, conformational changes in SRP that alter the actual FRET

efficiency will also change the E* value, and the trend of the changes with different binding partners will be the same. FRET histograms were obtained by 1D projection of the 2D E*-S histograms onto the E* axis. In this context, we used E* in this study to demonstrate the relative conformational change in SRP induced by its binding partners.

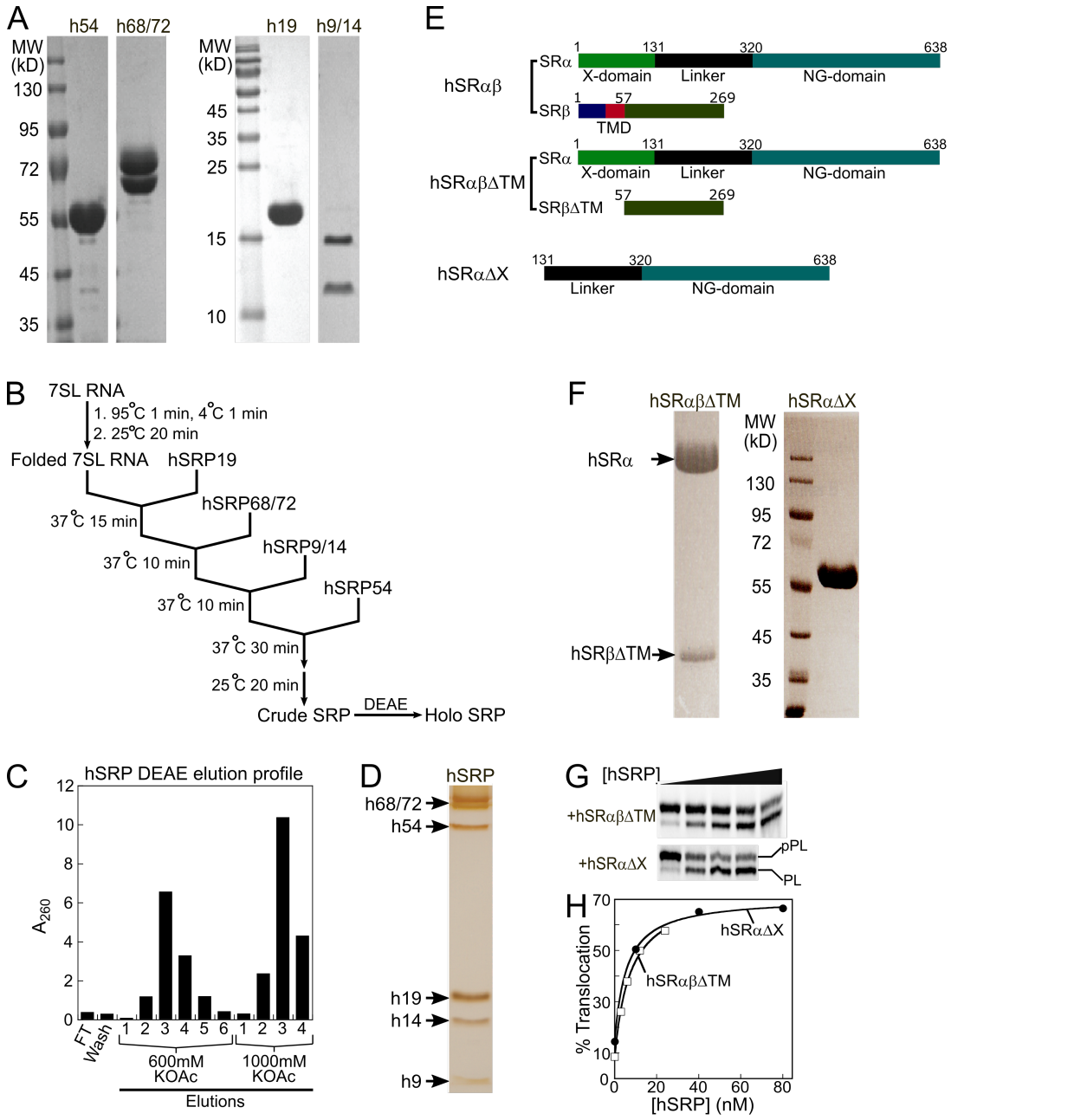

Figure S1. Large scale reconstitution of human SRP and SR. **(A)** Visualization of purified human SRP proteins by SDS-PAGE and Coomassie blue staining. **(B)** Outline of human SRP assembly based on modifications of published procedures (3, 4). SRP proteins were ultracentrifuged at 100,000 rpm in TLA100 rotor for 30 minutes to remove aggregates prior to assembly. SRP RNA was refolded by heating at 95 °C for 1 minute and snap cooling on ice for 1 minute, followed by addition of 0.25 volume of 5X Binding Buffer (100 mM Tris-HCl (pH 7.5), 1.5 M KOAc, 25 mM $Mg(OAc)_2$, 20 mM DTT, and 50% glycerol) and incubation at room temperature for 20 minutes. A typical 600 µL assembly reaction

contained 300 µL of 1XHKMN buffer (50 mM KHEPES (pH 7.5), 500 mM KOAc, 5 mM $Mg(OAc)_2$, 1 mM DTT, and 0.02% Nikkol) and the remainder with SRP proteins and RNA in 1X Binding Buffer. Refolded SRP RNA at a final concentration of 2.5 µM was first incubated with 4-6 µM hSRP19 at 37 °C for 15 minutes, followed by addition of 2.5 µM hSRP68/72 and 4 µM hSRP9/14 and an additional 10 minute incubation. 4 µM hSRP54 was added last, and the assembly mixture was incubated at 37 °C for 30 minutes and then at room temperature for 20 minutes. The assembly reaction was chilled on ice and diluted with 0.6 volume of Dilution Buffer (50 mM KHEPES (pH 7.5), 5 mM $Mg(OAc)_2$, 1 mM DTT, 0.01% Nikkol, and 20% glycerol). **(C)** A representative A_{260} profile of the purification of assembled hSRP using a DEAE-Sephacel column. The assembly mixture from part **B** was centrifuged at 18,000g for 5 minutes to remove large aggregates and loaded twice on 180 µl DEAE-sephacel resin pre-equilibrated in 20CV of Equilibration Buffer (50 mM KHEPES (pH 7.5), 250 mM KOAc, 3 mM $Mg(OAc)_2$, 0.5 mM EDTA, 1 mM DTT, 0.01% Nikkol, and 10% glycerol). The resin was washed with 5CV of Wash Buffer (50 mM KHEPES (pH 7.5), 350 mM KOAc, 4 mM $Mg(OAc)_2$, 0.5 mM EDTA, 1 mM DTT, 0.01% Nikkol, and 10% glycerol). Holo-SRP was eluted using 80 µl E600 Buffer (50 mM KHEPES (pH 7.5), 600 mM KOAc, 6.5 mM $Mg(OAc)_2$, 0.5 mM EDTA, 1 mM DTT, 0.01% Nikkol, and 10% glycerol) per fraction. Incompletely assembled SRP was eluted with E1000 Buffer (50 mM KHEPES (pH 7.5), 1000 mM KOAc, 6.5 mM $Mg(OAc)_2$, 0.5 mM EDTA, 1 mM DTT, 0.01% Nikkol, and 10% glycerol). Peak fractions containing SRP were collected based on A_{260} readings. FT denotes Flow-through. **(D)** Visualization of purified Holo-SRP by SDS-PAGE and silver staining. **(E)** Schematic of the hSR constructs used in this work. **(F)** Visualization of purified hSRαβΔTM and hSRαΔX by SDS-PAGE and Coomassie blue staining. **(G)** Representative co-translational targeting and translocation of preprolactin (pPL) mediated by reconstituted hSRP and hSR. pPL was translated in wheat germ extract in the presence of ^{35}S-methionine, hSRP and hSR, and salt-washed/trypsinized rough ER microsomes (TKRM). Reactions were stopped after 30-40 minutes and analyzed by SDS-PAGE and autoradiography. **(H)** Quantification of the data in part **G** for reactions with hSRαβΔTM (□) and hSRαΔX (●).

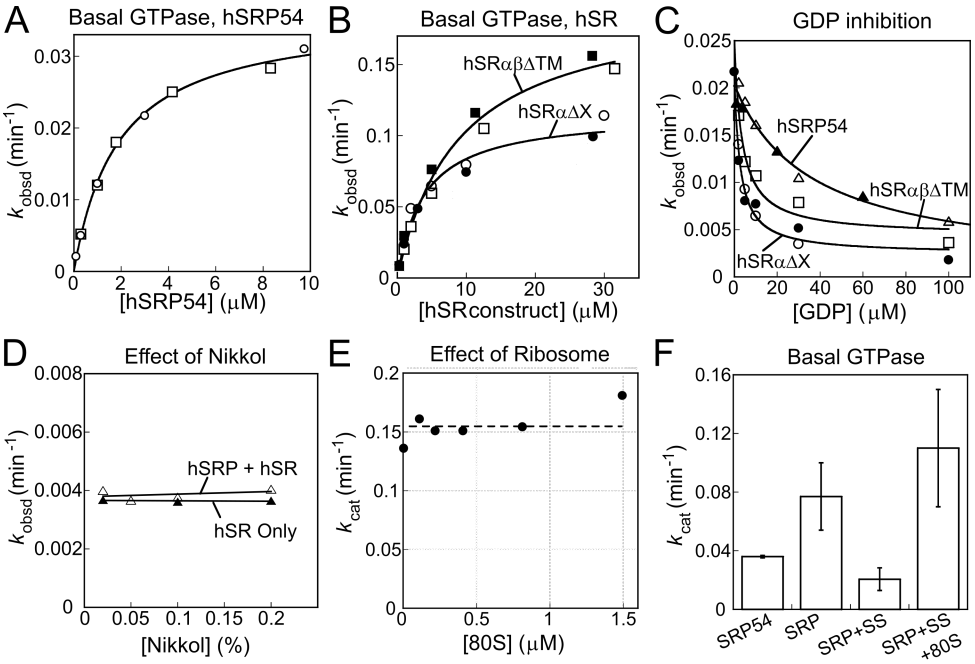

Figure S2. Basal GTPase activities of hSRP, hSR, and their controls. **(A, B)** The basal GTPase reactions of hSRP54 **(A)**, hSRαβΔTM (**B**, □■), and hSRαΔX (**B**, ○●) were measured under single-turnover conditions with trace γ-^{32}P-GTP and indicated concentrations of proteins. The lines are fits of the data to Eq. 1 in the SI Methods, and the obtained rate constants are summarized in Fig. 1B. **(C)** Inhibition assay to measure the binding of GDP to hSRP54 (Δ,▲), hSRαβΔTM (□), and hSRαΔX (○,●). Observed rate constants were measured under single-turnover conditions using 1 μM hSRP54 or hSR and indicated concentrations of GDP. The lines are fits of the data to Eq. 3, and the values of K_i are summarized in Fig. 1B. Open and closed symbols denote the data from two independent measurements. **(D)** Increasing concentrations of Nikkol (up to 0.2%) do not affect the basal GTPase activity of hSR (▲), nor the stimulated GTPase reaction of hSRP with hSR (Δ). **(E)** The basal GTPase activity of hSR was unaffected by the ribosome. The intrinsic GTPase activity of hSR was measured under k_{cat} conditions with increasing concentrations of 80S. **(F)** Signal sequence and ribosome did not substantially stimulate the basal GTPase activity of hSRP.

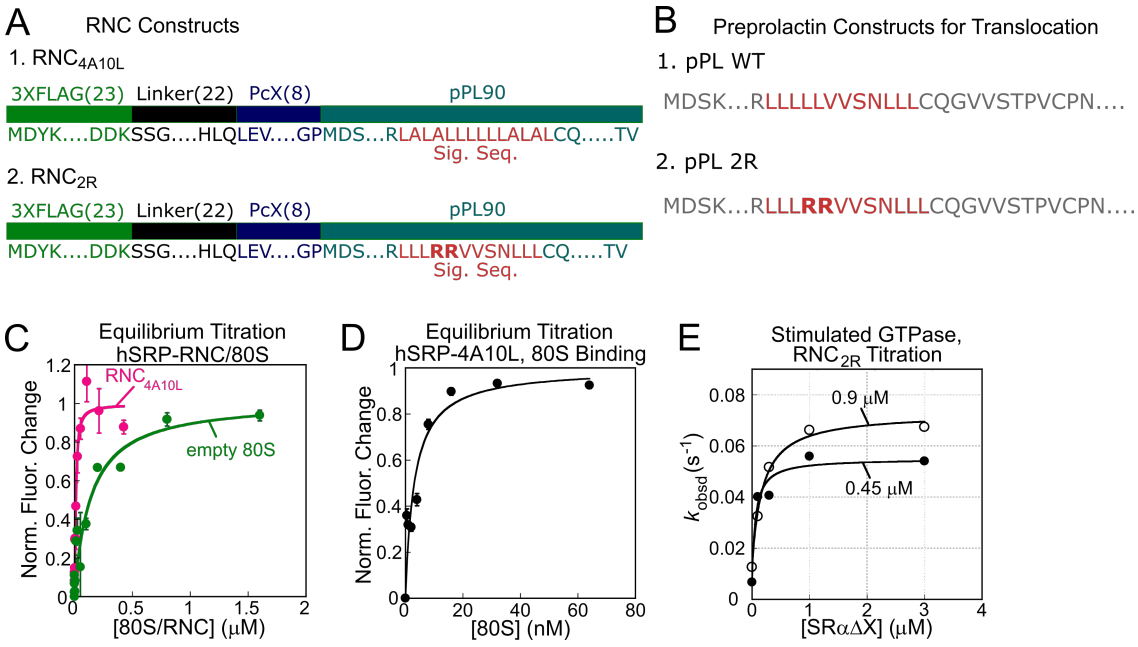

Figure S3. Schematic depiction of substrates used in this work and measurement of hSRP binding to ribosomal complexes. **(A)** The nascent chain of RNCs were based on the first 90 amino acids of preprolactin (pPL). An N-terminal 3xFLAG tag allows for affinity purification, and is followed by a 20 amino acid flexible linker and a PreScission protease site (PcX) for removing the affinity tag after purification. The pPL signal sequence was mutated to 4A10L or 2R to generate a correct and an incorrect substrate for SRP. **(B)** N-terminal sequences of full-length pPL, a model substrate for SRP-dependent co-translational targeting and translocation, and a 2R mutant of pPL as a negative control. Red highlights the wildtype or mutant signal sequence. **(C)** Equilibrium titration to measure the binding of hSRP to RNC_{4A10L} and the 80S ribosome. Measurements were based on Microscale Thermophoresis (MST) using 20 nM of Cy3B labeled hSRP and indicated concentrations of purified 80S or RNC_{4A10L}. The lines are fits of the data to Eq. 8, and gave K_d values of 5.1 ± 2.0 nM and 120 ± 29 nM for RNC_{4A10L} and 80S, respectively. **(D)** Equilibrium titration to measure the binding of signal sequence fused hSRP to the 80S ribosome using MST. The data was fit to Eq. 8 and gave a K_d value of 3.1 ± 1.0 nM. All data are presented as mean ± S.D., with n = 3. **(E)** GTPase activity measured with increasing concentrations of RNC_{2R}. Reciprocally stimulated GTPase reaction between hSRP and hSRαΔX was measured in the presence of either 0.45 μM (closed circle) or 0.9 μM (open circle) of RNC_{2R}.

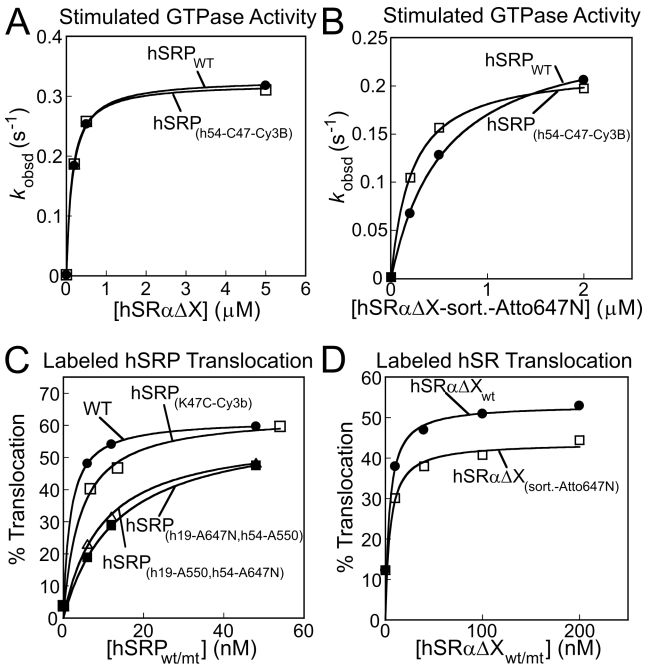

Figure S4. Fluorescence labeling does not substantially affect the activity of hSRP and hSR. **(A**, **B)** Reciprocally stimulated GTPase reactions between hSRP and hSR were measured as in Fig. 2A with wildtype hSRP and hSRαΔX (**A**, open), Cy3B-labeled hSRP and hSRαΔX (**A**, closed), hSRP and ATTO 647N-labeled hSRαΔX (**B**, closed), and the combination of dye-labeled hSRP and hSR (**B**, open). Note the different scales in **A** and **B**. **(C**, **D)** Co-translational targeting and translocation of pPL was measured as in Fig. S1H with fluorescently labeled hSRP (**C**) and hSR (**D**). The reactions in **c** contained 200 nM hSR. The reactions in **D** used 30 nM hSRP.

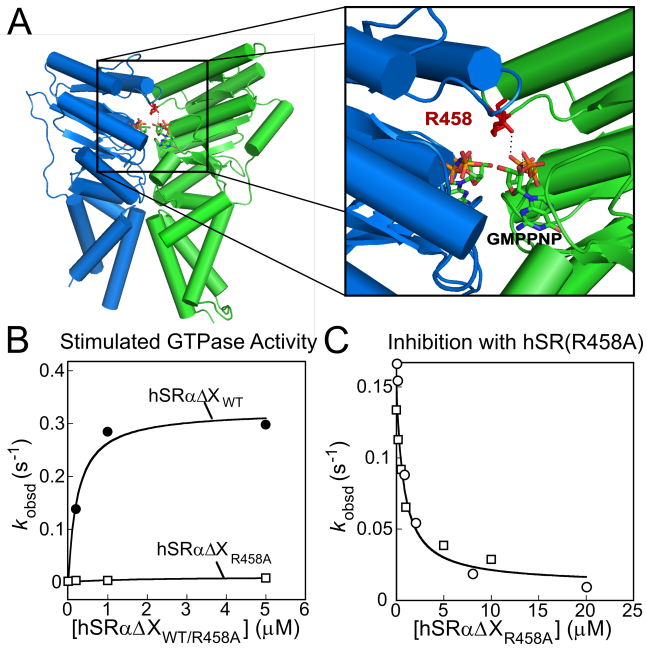

Figure S5. Characterization of the mutant hSR(R458A). **(A)** R458 in hSRα is highlighted in the crystal structure of the NG-domain complex between hSRP54 (*blue*) and hSRα (*green*; PDB 5L3Q) (19). The bound nucleotides are in *stick*, and the dotted line shows the hydrogen bond between R458 and the γ-phosphate of GMPPNP. **(B)** Reciprocally stimulated GTPase reaction of hSRP with hSRαΔX (closed symbols) and hSRαΔX(R458A) (open symbols), measured as in Fig. 2A. **(C)** hSRαΔX(R458A) potently inhibits the interaction between hSRP and hSRαΔX. Reciprocally stimulated GTPase reactions were measured with 0.2 μM hSRP and 0.5 μM hSRαΔX in the presence of the indicated concentrations of mutant hSRαΔX (R458A). The data were fit to Eq. 4 in the SI Methods, which gave an apparent inhibition constant of K_i = 83 nM. '□' and '○' denote the data from two independent measurements.

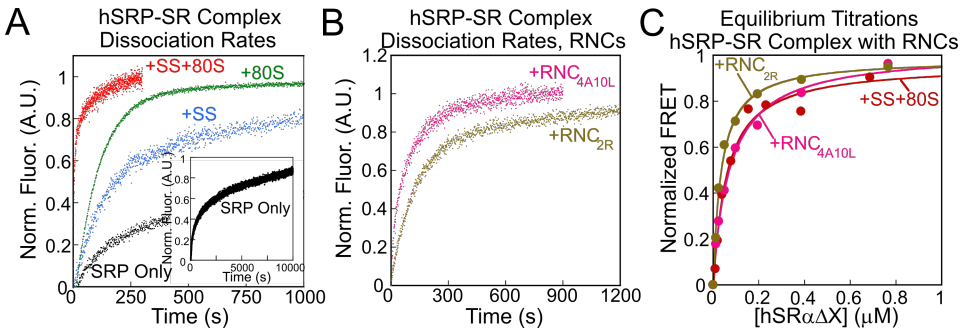

Figure S6. Additional FRET measurements of the hSRP-SR interaction. **(A)** Representative time traces of hSRP-hSR dissociation in the presence of the indicated SRP ligands. 12.5 nM hSRP or hSRP-4A10L was pre-incubated with labeled hSR (hSR*) to allow their complex formation, and unlabeled hSR was added to initiate complex dissociation. The following concentrations of labeled and unlabeled hSR were used: 2 μM hSR* and 10 μM hSR for the reaction with hSRP only, 0.25 μM hSR* and 2.5 μM hSR in the presence of 80S (300 nM), 2 μM hSR* and 8 μM hSR for hSRP-4A10L, and 75 nM hSR* and 375 nM hSR for hSRP-4A10L bound to 80S (40 nM). The data were fit to double exponential functions, and the weighted sum of the observed rate constants were reported in Table 2. **(B)** Representative time traces of hSRP-SR dissociation in the presence of RNCs, measured as in part **A**. The following concentrations of labeled and unlabeled hSR were used: 160 nM hSR* and 0.8 μM hSR for hSRP bound to RNC_{4A10L}, and 400 nM hSR* and 4 μM hSR for hSRP bound to RNC_{2R}. **(C)** Equilibrium titrations to measure the stability of the hSRP-SR complex in the presence of RNCs. Titrations were carried out under the same conditions as in Fig. 3C, except that 300 nM RNCs were used instead of ribosomes.

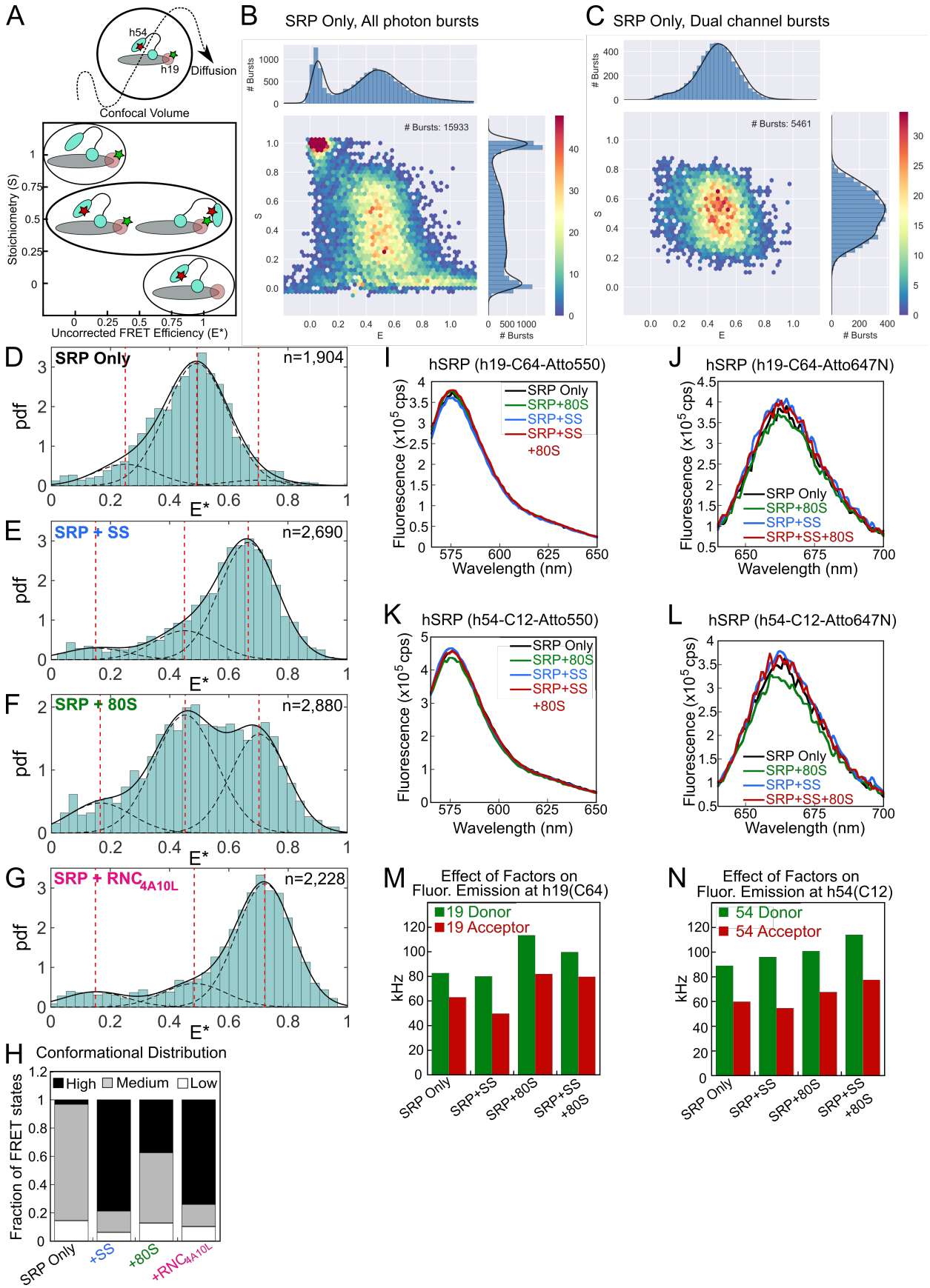
A
h54
h19
Diffusion
Confocal Volume
Stoichiometry (S)
Uncorrected FRET Efficiency (E*)
B
SRP Only, All photon bursts
Bursts
Bursts: 15933
S
E
C
SRP Only, Dual channel bursts
Bursts: 5461
D
SRP Only
n=1,904
pdf
E*
E
SRP + SS
n=2,690
F
SRP + 80S
n=2,880
G
SRP + RNC4A10L
n=2,228
H
Conformational Distribution
High
Medium
Low
Fraction of FRET states
SRP Only
+SS
+80S
+RNC4A10L
I
hSRP (h19-C64-Atto550)
SRP Only
SRP+80S
SRP+SS
SRP+SS +80S
Fluorescence (x10^5 cps)
Wavelength (nm)
J
hSRP (h19-C64-Atto647N)
SRP+SS+80S
K
hSRP (h54-C12-Atto550)
L
hSRP (h54-C12-Atto647N)
M
Effect of Factors on Fluor. Emission at h19(C64)
19 Donor
19 Acceptor
kHz
N
Effect of Factors on Fluor. Emission at h54(C12)
54 Donor
54 Acceptor

Figure S7. Schematic and control experiments for smFRET measurements. **(A)** Schematic depiction of the fluorescence-aided molecule sorting measurements using Alternating Laser Excitation Spectroscopy (ALEX). Fluorescently labeled SRPs diffusing through a femtoliter-scale observation volume are alternatively excited with donor (green) and acceptor (red) excitation lasers, and fluorescence emission from both the donor and acceptor dyes are measured to calculate donor-acceptor stoichiometry (S) and uncorrected FRET efficiency (E*) to generate a 2-D E*-S plot. This allows optical purification of the doubly labeled particles with both donor and acceptor dyes (S ~ 0.5), and 1D-projection of the doubly labeled population onto the E* axis generates the FRET histogram (15). **(B-C)** Representative 2-D E*-S plots for free hSRP labeled with ATTO-550 at SRP19(C64) and ATTO-647N at SRP54(C12). Panel **B** shows all the data from the measurement, while panel **C** shows the data for doubly labeled species after optical purification. **(D-G)** FRET histograms for hSRP, labeled with ATTO-550 at SRP54(C12) and ATTO-647N at SRP19(C64), with various binding partners. **(H)** Summary of the fraction of hSRPs containing the SRP54-ATTO550/SRP19-ATTO647N pair in the Low, Medium, and High-FRET populations from the data in **D-G**. Compared to the SRP19-ATTO550/SRP54-ATTO647N pair (Fig. 6), switching the position of donor and acceptor dyes did not significantly affect the FRET distribution of hSRP and its regulation by various ligands. Although the High-FRET state was slightly more populated with the SRP19-ATTO647N/SRP54-ATTO550 dye pair, the ribosome and signal sequence-induced changes in FRET distributions are the same between the two dye pairs. **(I-N)** Steady state fluorescence measurements (**I-L**) and median photon emission rate measurements on the ALEX setup (**M, N**) detected no significant effects of the various SRP ligands on the fluorescence of donor and acceptor dyes labeled at either SRP position.

Table S1. Summary of the rate constants from measurements of the stimulated GTPase reaction between human SRP and SR. N.D, not detectable. Values are reported as mean ± S.D., with n ≥ 2.

	hSRαβΔTM		hSRαΔX	
	k_{cat} (s^{-1})	k_{cat}/K_m ($M^{-1}s^{-1}$)	k_{cat} (s^{-1})	k_{cat}/K_m ($M^{-1}s^{-1}$)
SRP Only	N.D.	N.D.	N.D.	N.D.
+SS	0.082 ± 0.018	$6.7(\pm0.53) \times 10^4$	0.087 ± 0.012	$8.3(\pm0.50) \times 10^4$
+80S	0.032 ± 0.00017	$1.5(\pm0.19) \times 10^5$	0.057 ± 0.012	$2.3(\pm0.28) \times 10^5$
+SS+80S	0.15 ± 0.008	$8.0(\pm3.0) \times 10^5$	0.21 ± 0.017	$2.5(\pm0.5) \times 10^6$

Table S2. Summary of the rate and equilibrium constants of the SRP-SR interaction measured using the FRET assay. Values are reported as mean ± S.D., with n ≥ 2.

	k_4 ($M^{-1}s^{-1}$)	k_{-4} (s^{-1})	K_d (k_{off}/k_{on}) (nM)	Measured K_d (nM)
SRP Only	$8.6(\pm4.1) \times 10^1$	$8.9(\pm0.14) \times 10^{-4}$	10350	*2460 ± 48
+SS	$8.4(\pm0.78) \times 10^3$	$3.3(\pm1.3) \times 10^{-3}$	393	326 ± 13
+80S	$1.6(\pm0.10) \times 10^5$	$9.1(\pm0.60) \times 10^{-3}$	57	64 ± 10
+SS+80S	$3.5(\pm0.50) \times 10^6$	$8.3(\pm1.1) \times 10^{-2}$	24	56 ± 13
RNC_{4A10L}	$1.0(\pm0.10) \times 10^6$	$1.7(\pm0.12) \times 10^{-2}$	17	77 ± 5
RNC_{2R}	$6.5(\pm0.76) \times 10^4$	$5.7(\pm1.0) \times 10^{-3}$	88	35 ± 4

* In the absence of ligands, the K_d value from the equilibrium titration is less accurate, because saturation could not be reached due to limitations in protein concentration, and because of difficulties in reaching equilibrium at low SR concentrations due to the slow assembly rates.

References

1. Gowda K*, et al.* (1998) Protein SRP54 of human signal recognition particle: cloning, expression, and comparative analysis of functional sites. *Gene* 207(2):197-207.
2. Walker KP, 3rd, Black SD, & Zwieb C (1995) Cooperative assembly of signal recognition particle RNA with protein SRP19. *Biochemistry* 34(37):11989-11997.
3. Mary C*, et al.* (2010) Residues in SRP9/14 essential for elongation arrest activity of the signal recognition particle define a positively charged functional domain on one side of the protein. *RNA* 16(5):969-979.
4. Huck L*, et al.* (2004) Conserved tertiary base pairing ensures proper RNA folding and efficient assembly of the signal recognition particle Alu domain. *Nucleic Acids Res* 32(16):4915-4924.
5. Menichelli E, Isel C, Oubridge C, & Nagai K (2007) Protein-induced conformational changes of RNA during the assembly of human signal recognition particle. *J Mol Biol* 367(1):187-203.
6. Travers KJ, Boyd N, & Herschlag D (2007) Low specificity of metal ion binding in the metal ion core of a folded RNA. *RNA* 13(8):1205-1213.
7. Sharma A, Mariappan M, Appathurai S, & Hegde RS (2010) In vitro dissection of protein translocation into the mammalian endoplasmic reticulum. *Methods Mol Biol* 619:339-363.
8. Voorhees RM & Hegde RS (2015) Structures of the scanning and engaged states of the mammalian SRP-ribosome complex. *Elife* 4.
9. Verma R, Oania RS, Kolawa NJ, & Deshaies RJ (2013) Cdc48/p97 promotes degradation of aberrant nascent polypeptides bound to the ribosome. *Elife* 2:e00308.
10. Zhang X, Kung S, & Shan SO (2008) Demonstration of a multistep mechanism for assembly of the SRP x SRP receptor complex: implications for the catalytic role of SRP RNA. *J Mol Biol* 381(3):581-593.
11. Guimaraes CP*, et al.* (2013) Site-specific C-terminal and internal loop labeling of proteins using sortase-mediated reactions. *Nat Protoc* 8(9):1787-1799.
12. Peluso P, Shan SO, Nock S, Herschlag D, & Walter P (2001) Role of SRP RNA in the GTPase cycles of Ffh and FtsY. *Biochemistry* 40(50):15224-15233.
13. Shan SO, Chandrasekar S, & Walter P (2007) Conformational changes in the GTPase modules of the signal reception particle and its receptor drive initiation of protein translocation. *J Cell Biol* 178(4):611-620.
14. Powers T & Walter P (1997) Co-translational protein targeting catalyzed by the Escherichia coli signal recognition particle and its receptor. *EMBO J* 16(16):4880-4886.
15. Kapanidis AN*, et al.* (2005) Alternating-laser excitation of single molecules. *Acc Chem Res* 38(7):523-533.
16. Kapanidis AN*, et al.* (2004) Fluorescence-aided molecule sorting: analysis of structure and interactions by alternating-laser excitation of single molecules. *Proc Natl Acad Sci U S A* 101(24):8936-8941.
17. Ingargiola A, Lerner E, Chung S, Weiss S, & Michalet X (2016) FRETBursts: An Open Source Toolkit for Analysis of Freely-Diffusing Single-Molecule FRET. *PLoS One* 11(8):e0160716.
18. Nir E*, et al.* (2006) Shot-noise limited single-molecule FRET histograms: comparison between theory and experiments. *J Phys Chem B* 110(44):22103-22124.
19. Wild K*, et al.* (2016) Structural Basis for Conserved Regulation and Adaptation of the Signal Recognition Particle Targeting Complex. *J Mol Biol* 428(14):2880-2897.